THE ROYAL SOCIETY

Two-dimensional Fourier analysis of the spongy medullary keratin of structurally coloured feather barbs

Richard O. Prum[1]*, Rodolfo Torres[2], Scott Williamson[1] and Jan Dyck[3]

[1]*Natural History Museum and Department of Ecology & Evolutionary Biology and* [2]*Department of Mathematics, University of Kansas, Lawrence, KS 66045-2454, USA* (*prum@ukans.edu; rtorres@math.ukans.edu*)
[3]*Institute of Population Biology, Universitetsparken 15, DK-2100 Copenhagen, Denmark*

We conducted two-dimensional (2D) discrete Fourier analyses of the spatial variation in refractive index of the spongy medullary keratin from four different colours of structurally coloured feather barbs from three species of bird: the rose-faced lovebird, *Agapornis roseicollis* (Psittacidae), the budgerigar, *Melopsittacus undulatus* (Psittacidae), and the Gouldian finch, *Poephila guttata* (Estrildidae). These results indicate that the spongy medullary keratin is a nanostructured tissue that functions as an array of coherent scatterers. The nanostructure of the medullary keratin is nearly uniform in all directions. The largest Fourier components of spatial variation in refractive index in the tissue are of the appropriate size to produce the observed colours by constructive interference alone. The peaks of the predicted reflectance spectra calculated from the 2D Fourier power spectra are congruent with the reflectance spectra measured by using microspectrophotometry. The alternative physical models for the production of these colours, the Rayleigh and Mie theories, hypothesize that medullary keratin is an incoherent array and that scattered waves are independent in phase. This assumption is falsified by the ring-like Fourier power spectra of these feathers, and the spacing of the scattering air vacuoles in the medullary keratin. Structural colours of avian feather barbs are produced by constructive interference of coherently scattered light waves from the optically heterogeneous matrix of keratin and air in the spongy medullary layer.

Keywords: constructive interference; feathers; Fourier analysis; structural colour

1. INTRODUCTION

Structural colours of organisms are produced by optical interactions of light with biological structures that are similar in size to the wavelengths of visible light. Colour-producing biological nanostructures are extremely diverse in composition, but most are unified by a common structural organization and physical mechanism. Most function as multilayer reflectors in which two or more media with different refractive indices are organized in alternating parallel layers (Land 1972; Macleod 1986). Multilayer reflectors produce colours by constructive interference among light waves scattered coherently from the interfaces between media of different refractive indices. Physical models of 'ideal' reflectors predict that the optical thickness (the refractive index × the actual thickness) of each layer should be equal to one-quarter of the wavelength of maximum reflectance (Land 1972; Macleod 1986). Such 'quarter-wave' stacks have been identified in structurally coloured tissues from many animal phyla (see, for example, Land 1972) and a diversity of plants (Lee 1997). Recent research has also documented that various 'non-ideal' systems, in which optical thickness of layers varies, can produce structural colours that may be functionally superior and adaptive for particular organisms (Parker *et al.* 1998).

*Author for correspondence.

However, there are colour-producing biological structures that lack lamellar organization and to which multilayer reflector models do not apply. Researchers have tried to use Bragg's Law for some structures in which the scatterers are organized into nearly crystalline arrays (see, for example, Durrer 1962; Durrer & Villiger 1966, 1970; Prum *et al.* 1994). However, these applications are only approximate: the size and distance between scatterers varies, and each scatterer is not negligibly small in diameter in comparison to visible light (Land 1972).

Current models are even less appropriate for biological structures in which the scatterers are in a quasi-random, less-than-perfect array, as in the structurally coloured avian feather barbs examined here. In fact, the distribution of the scattering air vacuoles in the medullary keratin of structurally coloured feather barbs is so random that these structural colours are generally hypothesized to be produced by incoherent Rayleigh or Mie scattering instead of by coherent constructive interference (see, for example, Fox 1976; Finger 1995).

Recently, we conducted a two-dimensional (2D) Fourier analysis of the medullary keratin of the brilliantly blue feather barbs of the plum-throated cotinga (*Cotinga maynana*) (Prum *et al.* 1998). Our findings demonstrated that, despite its lack of lamellar or crystal-like organization, the spatial variation in refractive index of the medullary keratin of *Cotinga* is highly nanostructured, and

Received 7 August 1998 *Accepted* 10 September 1998

that this nanostructure is approximately the correct size to produce the observed blue hue by constructive interference alone. Our results also indicated that the physical conditions required for the alternative incoherent scattering mechanisms, Rayleigh or Mie scattering, are not met by this tissue (Prum *et al.* 1998).

In this paper, we present more detailed Fourier analyses of feather barbs from several species that produce a variety of different colours with a variety of medullary structures. Our goals are to test the current alternative hypotheses for the production of these colours (constructive interference compared with Rayleigh and Mie scattering), and to present a new method for the analysis of colour production by biological structures that lack the lamellar or crystalline organization assumed by most models of coherent light scattering. Specifically, we apply a 2D Fourier analysis, derived from an electromagnetic physical model of light scattering by the transparent human cornea (Benedek 1971), to document the periodicity of spatial variation in refractive index in the colour-producing keratin matrix of the medullary layer of structurally coloured feather barbs.

(a) *Structural colours of feather barbs*

There are three different classes of colour-producing structures in feathers. The first is unspecialized, unpigmented feather keratin, which produces white by incoherent scattering of all visible light waves. The second class includes structurally coloured feather barbules, which produce generally iridescent structural colours by constructive interference from arrays of melanin granules and/or air vacuoles suspended in the barbule keratin (Dyck 1971*b*, 1976, 1978, 1987; Lucas & Stettenheim 1972; Fox 1976; Durrer 1986). Here, 'iridescence' refers only to colours that change hue with the angle of incidence or observation.

The third class of colour-producing feather structures includes the specialized, spongy, medullary layer of feather barbs, which are the sole subject of the analyses presented here. The spongy medullary layer is composed of a matrix of keratin rods and air vacuoles of varying shapes and sizes around a basal layer of melanin granules that often surround a large air-filled nuclear vacuole (Auber 1957; Dyck 1971*a*,*b*, 1976, 1978; Lucas & Stettenheim 1972; Fox 1976; Durrer 1986). This spongy, medullary keratin matrix is absent in non-colour-producing feather barbs (Dyck 1978). The medullary keratin matrices differ from multilayer reflectors (Land 1972) in that they are not organized around any particular axis or plane of symmetry (Auber 1957; Dyck 1971*a*,*b*, 1976, 1978; Lucas & Stettenheim 1972; Fox 1976). Although medullary keratin varies in size, extent, and distribution on the obverse and reverse surfaces (upper and lower, respectively) of feather barbs (see, for example, Auber 1957; Andersson 1996, 1998), the matrix itself is not organized into layers or a crystal-like array or oriented in any predictable way to the surface of the feather or to the incident light.

Structurally coloured feather barbs produce generally non-iridescent blue, violet, turquoise, and ultraviolet (UV) hues. These colours are broadly distributed among birds, and must have arisen numerous times independently within the phylogenetic history of Aves (Auber 1957; Dyck 1971*a*,*b*, 1976, 1978; Durrer 1986; Finger *et al.* 1992; Finger 1995; Andersson 1996). In combination with yellow carotenoid pigments in the barb cortex, structural barb colours are an essential component of most green bird plumages (Fox 1976; Dyck 1978).

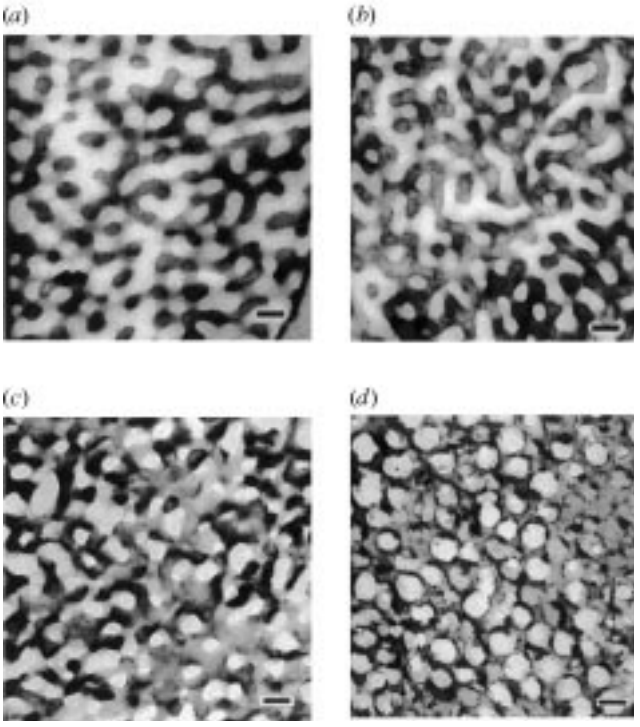

Figure 1. Transmission electron micrographs of the spongy medullary keratin matrix from feather barbs of (*a*) blue *Agapornis roseicollis*, (*b*) green *Agapornis roseicollis*, (*c*) light blue *Melopsittacus undulatus* and (*d*) violet *Poephila guttata*. Scale bars, 200 nm.

(b) *Alternative hypotheses of structural colour production in feather barbs*

Despite more than a century of research (reviewed in Dyck 1971*a*; Fox 1976), the physical mechanism of colour production by feather barbs is still being debated (Dyck 1971*a*,*b*, 1978; Fox 1976; Finger 1995; Andersson 1996). These colours are produced by light-scattering at the interfaces of the keratin and air, which differ in refractive index (RI=1.54 and 1.00, respectively; Dyck 1971*a*). The alternative hypotheses differ in whether the colours result from incoherent differential scattering of visible wavelengths or from the phase interactions among coherently scattered waves.

Rayleigh scattering has been the primary, accepted explanation of structural colours of feather barbs for nearly a century (Häcker & Meyer 1902; see reviews in Dyck 1971*a*; Fox 1976), and is cited in all general ornithological texts and reference works (e.g. Campbell & Lack 1985; Brooke & Birkhead 1991; Gill 1995). The term 'Rayleigh scattering' has been used confusingly by physicists to refer to a number of different light-scattering phenomena (Young 1982) but is now generally agreed to refer to an approximate model of light scattering by particles that are smaller than the wavelength of visible light, including small spheres or molecules (van de Hulst 1981; Young 1982; Bohren & Huffman 1983). The Rayleigh model predicts that the scattering efficiency of a particle of a given size will be inversely related to the fourth

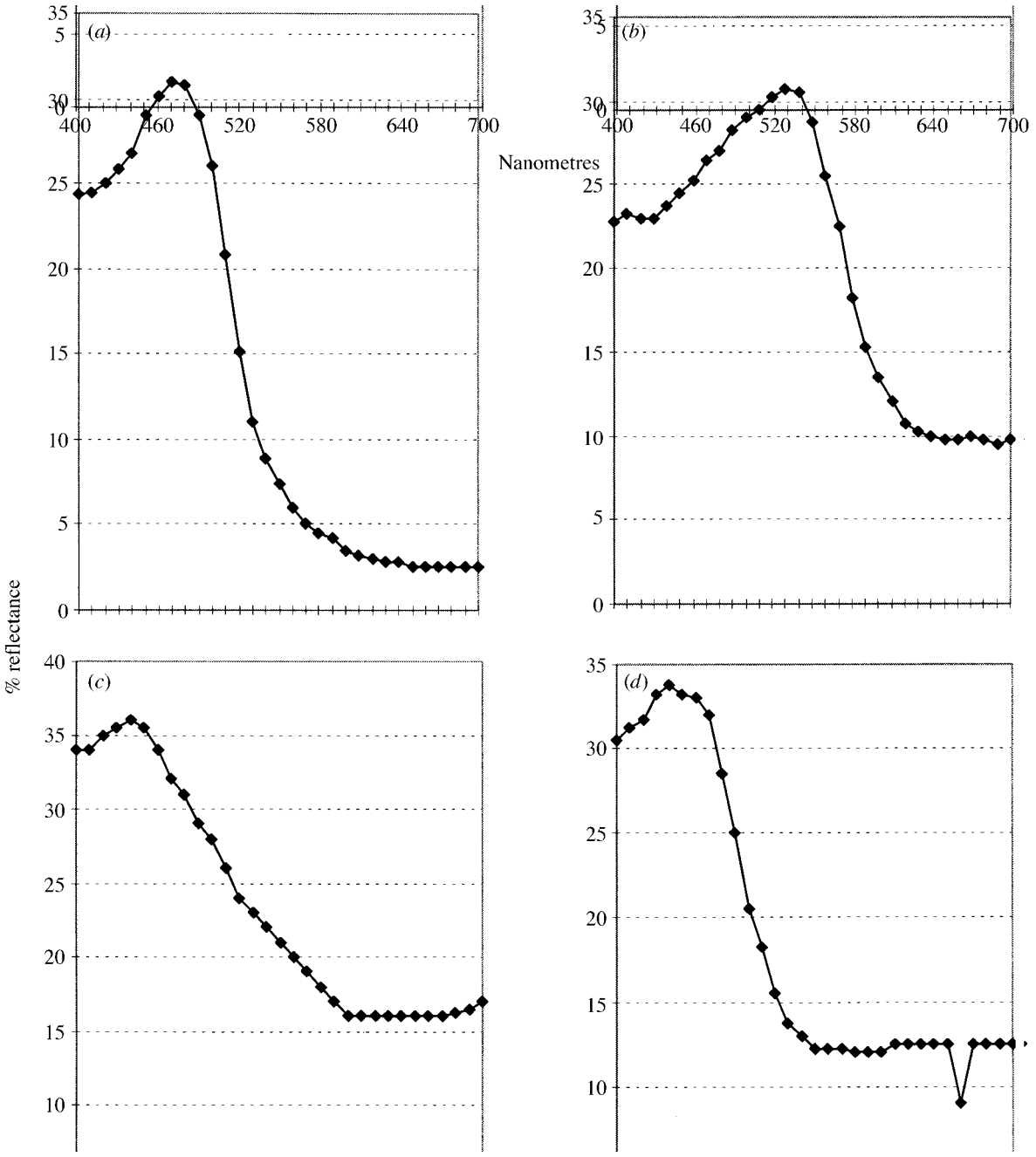

Figure 2. Reflectance spectra of feather barbs of (*a*) blue *Agapornis roseicollis*, (*b*) green *Agapornis roseicollis* with the yellow carotenoid pigment removed, (*c*) light blue *Melopsittacus undulatus* (Finger 1995), and (*d*) violet *Poephila guttata*.

power of the wavelength: Rayleigh's inverse fourth power law. Accordingly, Rayleigh scattering should produce blue, violet, or UV colours, depending on the size of the scatterers. Rayleigh scattering can only produce colours from the smaller end of the visible spectrum, because larger particles would scatter all wavelengths of light with equivalent efficiency, creating a white appearance.

Recently, Mie scattering, in combination with cortical filtering, has been proposed as an alternative explanation of structural colour production by feather barbs (Finger 1995). Mie theory is an exact electromagnetic model of scattering by an isolated homogeneous spherical particle (van de Hulst 1981; Bohren & Huffman 1983). Mie and Rayleigh theory are not distinct models: Mie theory reduces to Rayleigh's inverse power law for particles smaller than the wavelength of visible light that are not strongly absorbing (van de Hulst 1981; Bohren & Huffman 1983).

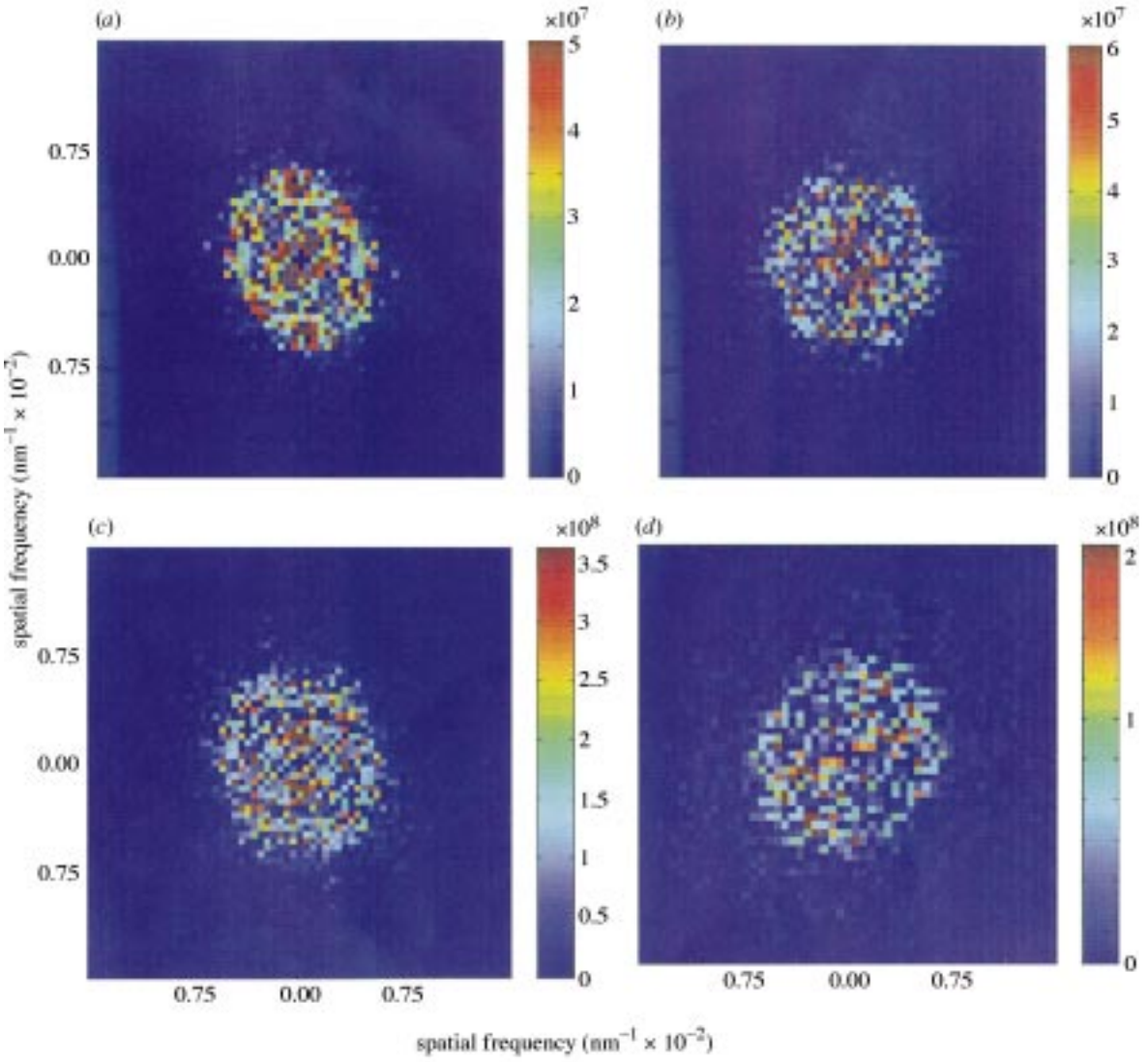

Figure 3. 2D Fourier power spectra of the spatial variation in refractive index in the spongy medullary keratin of (*a*) blue *Agapornis roseicollis*, (*b*) green *Agapornis roseicollis*, (*c*) light blue *Melopsittacus undulatus*, and (*d*) violet *Poephila guttata*. The spatial frequency and direction of each power-spectrum value are given by the length and direction, respectively, of a vector from the origin to that point. The magnitude of each power spectrum value is given by the colour (scale bars on right).

Both Mie and Rayleigh theory are models of incoherent light scattering. An array of scatterers is considered 'incoherent' if the phase relations among the light waves scattered by the array can be ignored in the description of its scattering behaviour (van de Hulst 1981; Bohren & Huffman 1983). An array is incoherent if its scatterers are separated by distances that are large in comparison with the wavelength of light concerned (van de Hulst 1981; Bohren & Huffman 1983). Incoherent scattering mechanisms hypothesize that structural colours of feather barbs are a consequence *only* of the size of the scatterers and the differential refractive index of the two media, and that the spatial distribution of the scatterers and the phase relations of scattered waves are irrelevant.

In contrast, the constructive interference model hypothesizes that the phase interactions among light waves scattered by the keratin–air matrix produce the structural colours of avian feather barbs (Raman 1935; Dyck 1971*a*,*b*, 1976). Constructive interference models take into account the phase relations among scattered waves, and are thus described as 'coherent' scattering models. The multilayer reflector (Land 1972) and Bragg reflection (Durrer 1962; Durrer & Villiger 1966, 1970; Prum *et al.* 1994) models are approximations of coherent scattering by arrays that are organized into lamellae or crystalline arrays, respectively.

According to the constructive interference model, scattered waves that are out of phase will destructively interfere and cancel out, whereas scattered waves that are in phase will constructively reinforce one another and be coherently reflected. The phase relations among scattered waves are determined by the size *and* spatial distribution of the scatterers (Benedek 1971; Dyck 1971*a*,*b*). The phase relations between two waves of the same wavelength scattered by different scatterers is determined by the difference between the distances travelled by each of the waves, called the path-length addition. For almost all wavelengths in a medium, a given path-length addition is a fraction, or non-integer multiple, of the wavelength. Such wavelengths will be out of phase after scattering, and will destructively interfere with one another and cancel out. However, those light waves that are near to

the size of the path-length addition (or an integer multiple of it) will travel a complete phase cycle over that distance, will be in phase with one another after scattering, and will reinforce one another to produce a wavelength-specific constructive reflection. The opportunity for constructive interference by a coherent medium is determined by the distribution of potential path-length additions, which is related to the periodicity of the spatial distribution of the scatterers (Benedek 1971). If the scatterers are randomly distributed, then path-length additions are also random, and scattering will be incoherent. However, periodic spatial relations among scatterers will produce a predictable distribution of path-length differences among scattered waves, and reinforcement of a limited set of wavelengths.

Constructive interference was first proposed as an explanation of structural colours in feather barbs by Raman (1935), who observed that individual feather barbs can be subtly iridescent. The constructive interference hypothesis was subsequently revived as an alternative to Rayleigh scattering in a series of publications by Dyck (1971*a*,*b*, 1976, 1978). Dyck documented that the reflectance spectra of many blue and green structurally coloured barbs showed discrete peaks in the visible spectrum, whereas the Rayleigh scattering model predicts a continued increase in scattering into the UV. Having falsified this prediction of the Rayleigh model, Dyck (1971*a*,*b*, 1976, 1978) presented the 'hollow cylinder' model, which hypothesizes that constructive interference from the ordered matrix of air vacuoles and keratin in the medullary layer produces the structural colours of feather barbs. Dyck (1971*a*,*b*, 1976, 1978) demonstrated that, for feather barbs of a variety of colours and species, the hue of a structural colour is strongly correlated with the size of the air vacuoles and keratin bars in the spongy medullary matrix. Although this evidence is supportive of constructive interference, Dyck could not address the fundamental question of whether the medullary keratin matrix is sufficiently ordered, or periodic, to produce wavelength-specific structural colours.

(c) *Discrete Fourier analysis and structural colour production*

In this paper, we address the following questions. (i) Is the structurally coloured spongy medullary keratin matrix sufficiently ordered to produce wavelength-specific colours by constructive interference? (ii) Is this matrix the appropriate size to produce the observed structural colours? (iii) Is the keratin matrix appropriately organized to produce structural colours by incoherent scattering (i.e. Rayleigh or Mie scattering)?

To examine these questions, we apply an explicit electromagnetic model of light scattering and transparency of the human cornea created by Benedek (1971). The vertebrate cornea is a quasi-random array of parallel collagen fibres (Maurice 1984). The cornea is transparent because the collagen fibres that compose it are very small and close together, resulting in destructive interference among all scattered wavelengths of visible light (Benedek 1971; Maurice 1984; Vaezy & Clark 1991, 1993). Previous research using Bragg's Law to analyse structural colour production by collagen arrays in the avian skin (Prum *et al.* 1994) led us to consider applying Benedek's theory of corneal transparency to structural colour production by the spongy medullary keratin matrix of feather barbs: an optically similar phenomenon on a different spatial scale.

Benedek (1971) developed an explicit, electromagnetic model for light scattering by an array of fibres. According to Benedek's theory, in a quasi-random array of scatterers (i.e. a less than perfect lattice), significant coherent reinforcement is predicted only for those light waves in the medium that are twice the size of the largest components of the Fourier transform of the spatial variation in refractive index (Benedek 1971). The discrete Fourier transform is a basic mathematical tool used to decompose a signal or image into different periodic components (Briggs & Henson 1995). Discrete data are transformed into a sum of component sine waves of different amplitudes and frequencies (Briggs & Henson 1995). The relative squared amplitudes of these component waves, called the Fourier power spectrum, express the contributions of each frequency of variation to the original data, and indicate which frequencies carry the most energy (Briggs & Henson 1995).

Benedek's theory predicts that the Fourier power spectrum of spatial variation in refractive index of a tissue will predict which wavelengths will be constructively reflected by that tissue. This is because the distribution of the Fourier coefficients of the spatial variation in refractive index is directly related to the distribution of the path-length additions experienced by light waves scattered by the tissue. Both 1D and 2D Fourier analysis have been used to analyse spatial variation in refractive index in optically transparent, opaque, and white tissues of the mammalian eye (Vaezy & Clark 1991, 1993; Gisselberg *et al.* 1991). Here, we apply 2D Fourier analysis to examine the relation between the spatial variation in refractive index in the medullary keratin matrix of the feather barbs and their structural colours. This application of Fourier analysis is derived independently from electromagnetic optical theory (Benedek 1971) and is completely unrelated to the traditional physical field of 'Fourier optics' in which the Fourier transform is used to describe the process of diffraction by a grating or the resolution of an image by a lens.

2. METHODS

(a) *Species sampled and observations*

We examined structurally coloured feather barbs of four different colours from three different species: blue and green contour feathers of the rose-faced lovebird, *Agapornis roseicollis* (Psittacidae); light blue contour feathers of a captive-bred blue mutant of the budgerigar, *Melopsittacus undulatus* (Psittacidae; KU 46538); and violet-purple contour feathers of the Gouldian finch, *Poephila guttata* (Estrildidae; KU 38025). Contour feathers were washed and prepared for microscopy and spectroscopy according to the methods of Dyck (1971*a*). Carotenoid pigments were extracted from the green *Agapornis* feathers as in Dyck (1971*a*). Transmission electron micrographs (TEM) were prepared for *Agapornis* as by Dyck (1971*a*), but TEMs of *Melopsittacus* and *Poephila* were taken with a Jeol JEM-1200 (figure 1).

Reflectance spectra of intact single feather barbs of *Agapornis* and *Poephila* were obtained with a Zeiss microspectrophotometer 01 using perpendicular incidence, according to the procedure of Dyck (1978). Percentage reflectance was calculated by dividing

the reflectance of the barb by the reflectance of a white standard for 30 different wavelengths at 10 nm intervals between 400 and 700 nm (figure 2). The reflectance spectrum for the light blue mutant *Melopsittacus* is from Finger (1995).

(b) *2D discrete Fourier analysis*

We used TEMs of the feather keratin matrix as an estimate of the spatial variation in refractive index of the tissue. Grey-scale variation in the images allowed us to distinguish between feather keratin and air vacuoles, and to estimate the spatial variation in refractive index in the spongy medullary keratin matrices.

TEM negatives of the spongy medullary keratin of the feather barbs of *Agapornis* (×20 000), *Melopsittacus* (×30 000) and *Poephila* (×30 000) were digitized at 300 dpi by means of a Hewlett-Packard Scanjet 3c (figure 1). The digitized TEM images were analysed with MATLAB (version 5.0; MATLAB Reference Guide 1992) on a Silicon Graphics Onyx workstation. The scale of each digitized image (nm per pixel) was calculated by measuring the number of pixels in the original TEM scale bar in the micrograph. Because the TEM sections are not infinitely thin, the TEMs do not accurately depict the sharp interfaces between the keratin and the air. Furthermore, the keratin structures frequently stain irregularly, producing spurious variation in this optically homogeneous medium. To control for these sources of error, the digitized TEMs were image processed to enhance the distinction between the keratin bars and air-filled vacuoles (i.e. the spatial function of refractive index), and to diminish grey-scale variation within each material (i.e. noise). The pixel intensity of each image was rescaled in relation to the original variance in intensity. Pixels more than one standard deviation away from the mean intensity value were assigned to 0 (black) or 1 (white) and the remaining variation was rescaled as a linear function between 0 and 1. To eliminate variation among different areas of the image, this variance rescaling was performed across the entire image on 30 pixel × 30 pixel blocks with five overlapping pixels between neighbouring blocks (i.e. block processing; Thompson & Shure 1995). Pixel intensity was then median-filtered: each pixel received the mean of the surrounding 4 pixel × 4 pixel matrix. The largest available square portion of the keratin matrix was then selected for analysis (between 600 and 625 pixels^2). Large-scale singularities in the images (e.g. cell boundaries or melanin granules) were avoided when possible, because analysis of larger-scale variation in structure of the feathers can disrupt the description of the nanoscale variation in refractive index of the medullary keratin matrix itself.

The mean refractive index of the tissue in each image was estimated by generating a 2-bin histogram of image density from the processed images (Thompson & Shure 1995). The frequency distributions of the darker and lighter pixels in the block-processed images were used to estimate the relative volume of keratin (RI = 1.54) and air (RI = 1.00) in the image; this relative volume was then used to calculate a weighted mean refractive index for the tissue (Dyck 1971*a*). These weighted means may underestimate the mean refractive index of the entire feather barb, because we did not include the completely keratinous barb cortex.

The numerical computation of the Fourier transform was done with the well-established 2D fast Fourier transform (FFT2) algorithm (Briggs & Henson 1995) in MATLAB (MATLAB Reference Guide 1992; Thompson & Shure 1995), which is a broadly accepted, standard tool for this kind of analysis. Because the tissue has no plane of symmetry and is randomly orientated to the surface of the barbs, the orientation of the image within the matrix is not important (see § 3, figure 3). We then calculated the 2D Fourier power spectrum (the distribution of the squares of the Fourier coefficients). The 2D Fourier power spectrum resolves the spatial variation in refractive index in the tissue into its periodic components in any direction from a given point (figure 3). Each value in the power spectrum reports the magnitude of the periodicity in the original data at a specific spatial frequency in a given direction from all points in the original image. The spatial frequency and direction of any given component in the power spectrum are given by the length and direction, respectively, of a vector from the origin to that point. The 2D Fourier power spectra were expressed in spatial frequency (nm^{-1}) by dividing the initial spatial frequency values by the length of the matrix (pixels in the matrix × nm per pixel). The four quadrants of each power-spectrum matrix were shifted to place the four original corners of the matrix in the centre, so that the frequency origin was in the centre of the image.

We produced predicted reflectance spectra (figure 4) based on the 2D Fourier power spectra of each tissue (figure 3), and the size and mean refractive index of the images. First, we produced an estimate of the percentage total Fourier power of component waves of different sizes by taking a radial mean of a series of 0.5 pixel radial intervals of spatial frequency (diameters) for a single quadrant of the power spectrum. (The power spectrum of a 2D Fourier analysis is itself 3D; the three dimensions depict the size, direction, and magnitude of component spatial frequencies). The values of the radial mean of the 2D power spectrum were then rescaled so that the total volume (and total energy) under the rotated radial mean power function was equal to unity. Next, the relative percentage total power of Fourier components of different sizes (over all directions) was estimated by calculating the volumes of radial segments, or shells, of the normalized, rotated, radial mean of the power spectrum. The inverse of the spatial frequency values were then multiplied by twice the mean refractive index of the medium and expressed in terms of wavelength (nm). The result is a theoretical prediction of the relative magnitude of coherent scattering, or constructive interference, by the tissue that is based entirely on the spatial variation in refractive index of the tissue.

3. RESULTS

(a) *Anatomy and microspectroscopy*

All of the feather barbs examined have an extensive layer of spongy, medullary keratin that is characterized by a network of keratin rods and air vacuoles (figure 1). As in other structurally coloured feather barbs (Auber 1957; Dyck 1971*a*,*b*, 1976, 1978; Lucas & Stettenheim 1972; Fox 1976; Durrer 1986), the keratin matrices have no planes of symmetry and are not orientated to the surface of the feather in any predictable manner.

The size and structure of the keratin matrices vary among the species examined. *Agapornis* and *Melopsittacus* both feature rod-like or columnar keratin bars with relatively uniform diameter, and less uniform air vacuoles of variable shape and diameter (figure 1*a*–*c*). This type of medullary structure (type f, fig. 27 of Dyck 1978) is known from other psittacids, leafbirds (Irenidae) (Dyck 1971*b*, 1978; Finger *et al.* 1992), *Coracias* rollers (Coraciidae; R. O. Prum, personal observation), and *Myiophonas* thrushes (Muscicapidae; Andersson 1996). In *Poephila*, the

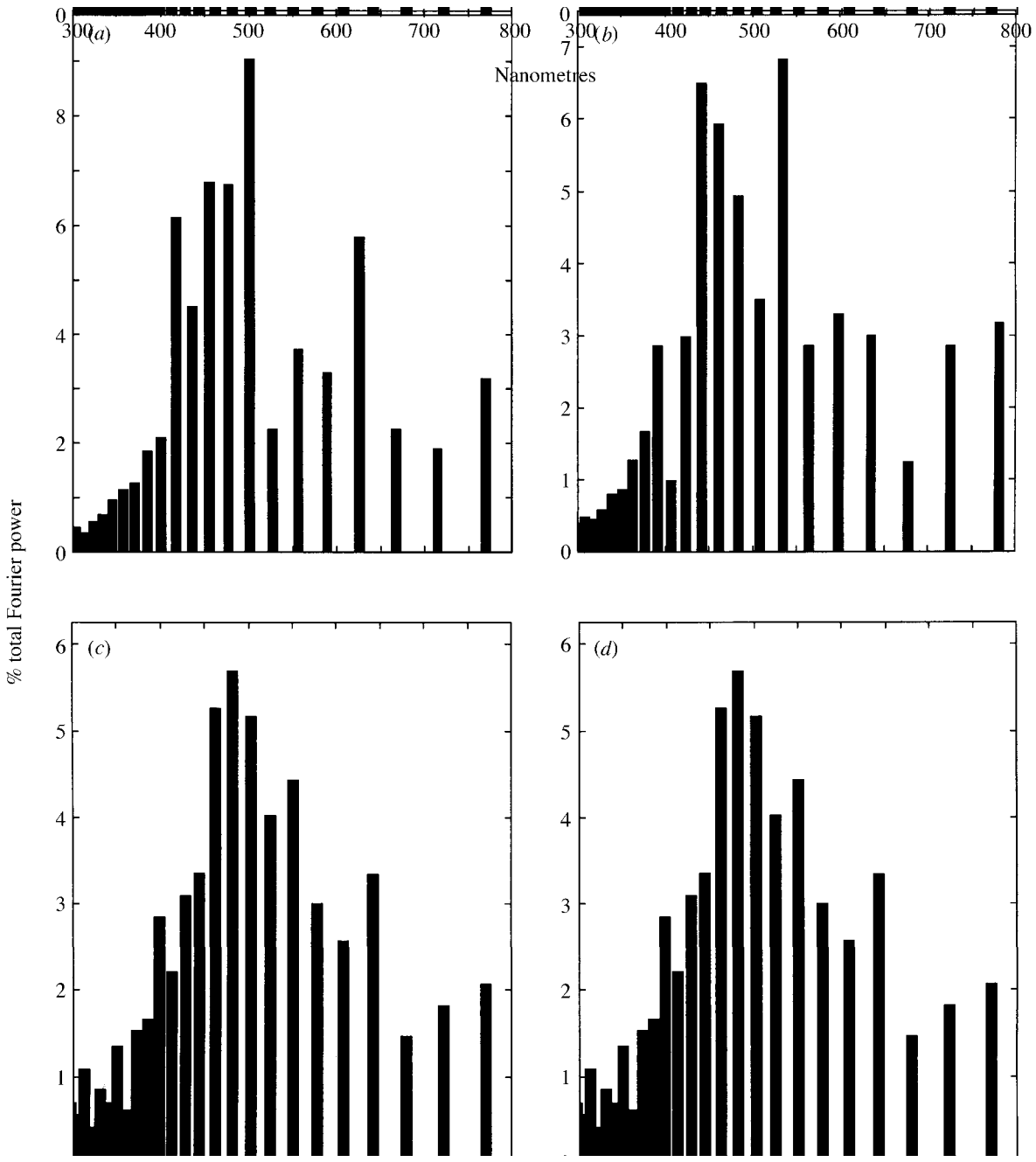

Figure 4. Predicted reflectance spectra based on the 2D Fourier power spectra of the medullary keratin of feather barbs from (*a*) blue *Agapornis roseicollis*, (*b*) green *Agapornis roseicollis* with the yellow carotenoid pigment removed, (*c*) light blue *Melopsittacus undulatus*, and (*d*) violet *Poephila guttata*. The predicted reflectance is given as percentage total Fourier power. (See § 2 for details.)

medullary structure is characterized by air vacuoles of uniform diameter and spacing with a continuous keratin medium in between (figure 1*d*). This type of organization (type e, fig. 27 of Dyck 1978) has also been found in *Cotinga* (Cotingidae; Dyck 1971*a*; Prum *et al.* 1998) and *Megalaima* barbets (Ramphastidae; Dyck 1978).

The reflectance spectra of all barbs examined showed discrete peaks in the visible spectrum between 440 and 540 nm (figure 2). The blue *Agapornis* barbs show a reflectance peak at 480 nm, whereas the green *Agapornis* barbs with the yellow carotenoid pigment extracted show a reflectance peak of 535 nm. The violet breast-feather barbs of *Poephila* show a distinct reflectance peak of 450 nm. The light blue barbs of domestic mutant *Melopsittacus* show a broad reflectance peak in the visible spectrum at about 440 nm (Finger 1995). The positions of the peaks in these reflectance spectra correspond well to the hue or appearance of the feather barbs. Although the reflectance peak of the light blue *Melopsittacus* barbs is a slightly smaller wavelength than that of the violet *Poephila* barbs, the differences between these reflectance spectra in the breadth of the peak, or chroma, also contributes to the observed differences in colour. The violet *Poephila* barbs strongly reflect a narrower band of lower visible

wavelengths, whereas the light blue *Melopsittacus* barbs show a broader reflectance spectrum.

(b) *2D Fourier analysis*

The 2D Fourier power spectra of all four spongy medullary tissues show a distinct disc pattern, with the largest power values near the centre of the disc and in a 'ring' surrounding the origin (figure 3). The clusters of high power values near the centre come from the lowest spatial frequencies and are caused by large-scale variations in the grey scale of the images. The main ring of larger power values indicates a predominant distribution of power at spatial frequencies that are the appropriate size scale to produce coherent reflections within the visible spectrum. The low power values at higher spatial frequencies indicate that these tissues have little periodic spatial variation at the smallest spatial scales. The power spectra indicate that the spatial variation in refractive index in the medullary keratin of these species is highly ordered on a nanoscale. Although some of the power spectra are slightly ovoid, the generally ring-like pattern indicates that this nanostructure is uniform in all directions (figure 3).

The 2D Fourier power spectra were used to predict the reflectance spectra of the feather barbs of each colour and species (figure 4; see § 2). In all four cases, the predicted reflectance spectra show distinct peaks in the visible spectrum, indicating that the vast majority of the spatial variation in refractive index is concentrated at spatial frequencies that should produce constructive reflections of light waves within the visible spectrum.

The peaks of the Fourier-predicted reflectance spectra are also generally congruent with the observed reflectance spectra of the same feather barbs (figures 2 and 4). Blue *Agapornis* barbs have a predicted reflectance peak of 500 nm (figure 4*a*) and an actual reflectance peak of 480 nm (figure 2*a*). Green *Agapornis* barbs with the yellow carotenoid pigment removed have a predicted reflectance peak of 535 nm (figure 4*b*), which is exactly congruent with the observed peak (figure 2*b*). Light blue *Melopsittacus* barbs have a predicted reflectance peak of 480 nm (figure 4*c*) and an observed peak of 440 nm (figure 2*c*). Violet *Poephila* barbs show a predicted reflectance peak of 425 nm (figure 4*d*) and an observed peak of 450 nm (figure 2*d*). The predicted spectra have peaks within 0–40 nm of the observed reflectance peaks.

The congruence between the observed and predicted reflectance peaks is striking given that there are no reasons, other than nanostructuring for colour production, to expect anything other than a flat distribution (i.e. white noise) or inverse exponential distribution (i.e. inverse frequency-dependent noise) in the Fourier power spectrum of the refractive index of the medullary keratin at this spatial scale.

(c) *Rayleigh and Mie scattering*

The reflectance spectra of the feather barbs examined had distinct peaks in the visible spectrum (figure 2) and did not conform to the predictions of Rayleigh's inverse fourth power law. As Dyck (1971*a*, 1978) concluded, this evidence falsifies a major prediction of the Rayleigh scattering model.

Futhermore, the physical conditions necessary for incoherent scattering assumed by Mie and Rayleigh theory are not present in the spongy medullary keratin of feather barbs. In the structurally coloured feather barbs observed here (and in all those previously described: Auber 1957; Dyck 1971*a*,*b*, 1976, 1978; Durrer 1986; Finger *et al.* 1992; Finger 1995; Andersson 1996), the light-scattering air vacuoles in the spongy medullary keratin matrix are much closer together than even the smallest wavelengths of visible light ($\ll$300 nm). Furthermore, the 2D Fourier power spectra from our analyses demonstrate that the heterogeneities in refractive index are not spatially independent of one another but highly ordered (figures 3 and 4). Mie and Rayleigh scattering are not appropriate models of structural colour production by avian feather barbs.

4. DISCUSSION

The 2D discrete Fourier analysis of the spongy medullary keratin of structurally coloured feather barbs demonstrates that these are highly ordered, nanostructured tissues. The nanostructure of the medullary keratin matrices is nearly uniform in all directions, and is close to the correct size to produce the observed colours by constructive interference. These results indicate that structural colours of feather barbs are produced by constructive interference of light waves scattered coherently by the interfaces between keratin and air in the spongy medullary layer of the barbs.

Previous results demonstrate that these same conclusions apply to the blue feather barbs of *Cotinga* (Prum *et al.* 1998). The results reported here indicate that these conclusions are generalizable to green, blue, and violet structural colours of feather barbs belonging to both major classes of medullary organization: those with keratin bars of relatively uniform diameter (e.g. *Agapornis*, *Melopsittacus*) (type f, fig. 27 of Dyck 1978). as well as those with air vacuoles of relatively uniform diameter (e.g. *Poephila*, *Cotinga*) (type e, fig. 27 of Dyck 1978). The same physical mechanism is also likely to apply to structurally UV-coloured feather barbs that have the former type of medullary organization (e.g. *Chalcopsitta*: Finger *et al.* 1992; *Myiophonus*: Andersson 1996, 1998).

Rayleigh scattering has been the predominant explanation of structural colour production by feather barbs for nearly a century (Häcker & Meyer 1902; see reviews in Dyck 1971*a*; Fox 1976), and is cited in all current general ornithology texts and references (e.g. Campbell & Lack 1985; Brooke & Birkhead 1991; Gill 1995). Our results demonstrate that a critical physical condition required for both Rayleigh and Mie scattering—incoherent scattering—is not met by any structurally coloured feather barbs, and is directly falsified by the ring-like Fourier power spectra of medullary feather keratin (figure 3).

Dyck (1971*a*,*b*, 1976, 1978) proposed the constructive interference (originally 'hollow cylinder') model as an alternative to Rayleigh scattering, but it received limited acceptance because of the lack of evidence demonstrating that the spongy medullary keratin is sufficiently ordered to produce coherent phase relations among scattered waves. However, advances in understanding light scattering by the transparent cornea demonstrate that tissues need not have a precise lamellar or lattice-like structure to produce predictable phase relations among scattered

light waves (Benedek 1971; Gisselberg *et al.* 1991; Vaezy & Clark 1991, 1993).

The spongy, medullary keratin of feather barbs belongs in a distinct class of structurally coloured tissues that function by constructive interference but which lack a lamellar or crystalline organization. The medullary keratin matrix functions by a physical mechanism similar to that of multilayer reflectors and Bragg arrays. Both systems have highly organized, nanoscale spatial variation in refractive index that produces coherent scattering. However, feather barbs differ strikingly from these other structures in that they are not organized or orientated on a larger spatial scale into layers or crystal-like lattices. The Fourier power spectra indicate that the nanostructure of the medullary keratin is nearly uniform in all directions (figure 3; Prum *et al.* 1998). As a consequence, changes in angle of incidence or observation do not change the overall distribution of path-length additions or the observed hue. In contrast to many structurally coloured tissues, feather barbs can produce brilliant hues that are nearly omnidirectional (Dyck 1971*a*, 1978). These functional attributes may explain the diversity, broad distribution, and multiple evolutionary origins of structurally coloured feather barbs in birds.

(a) *Fourier analysis and constructive interference*

Developed initially for the study of transparency (Benedek 1971; Gisselberg *et al.* 1991; Vaezy & Clark 1991, 1993, 1995; Vaezy *et al.* 1995), these Fourier techniques are exactly suited to the analysis of coherently scattering by biological tissues, especially structures that cannot be accurately modelled as multilayer reflectors. These include some iridescent avian feather barbules (Durrer 1986), vertebrate dermal collagen arrays (Prum *et al.* 1994), vertebrate and invertebrate iriphores (see, for example, Bagnara & Hadley 1973), and the mammalian tapetum lucidum (Land 1972). Furthermore, 1D or 2D Fourier techniques should also converge on current methods of analysing multilayer reflectors (Macleod 1986), such as those in the invertebrate exoskeleton (Fox 1976; Neville 1993; Parker *et al.* 1998) and structurally coloured plants (Lee 1997).

Previous discrete Fourier analyses by Vaezy, Clark and colleagues have focused on determining whether various tissues produce coherent scattering within the visible spectrum (Gisselberg *et al.* 1991; Vaezy & Clark 1991, 1993, 1995; Vaezy *et al.* 1995). We have been able to achieve finer resolution of spatial variations in refractive index by increasing the size of the images analysed from 256 pixels^2 to greater than 600 pixels^2.

We have made another analytical advance over previous studies. Vaezy, Clark and colleagues used a radial mean of the 2D Fourier power spectrum as the summary of the distribution of energy across various spatial frequencies (Gisselberg *et al.* 1991; Vaezy & Clark 1991, 1993, 1995; Vaezy *et al.* 1995). This method is an accurate way to estimate the distribution of the distance between scatterers, but it is not an accurate way to predict the reflectance spectrum of a tissue. The 'power' of the power spectrum is equal to its volume (the sum of all power spectrum values). Because the radial mean of the 2D power spectrum has no volume, the radial mean values do not express the differential contribution of each spatial frequency to the total *magnitude* of scattering by the heterogeneities in refractive index of the tissue. The *magnitude* of scattering by component spatial frequencies is related to the *power* or volume of those components in the power spectrum. We therefore calculated the volumes of cylinders, or shells, for increments of spatial frequency from the normalized, rotated radial mean of the 2D power spectrum to estimate more accurately the relative percentage of total power contributed by each interval of spatial frequency. In essence, the power values from the radial mean of the 2D power spectrum must be weighted by their distances from the origin to calculate the volumes of the shells they circumscribe. This distribution yields a more accurate description of the reflectance spectra of the tissues. This result explains why the high power values at small spatial frequencies near the origin of the power spectrum do not contribute substantially to the magnitude of scattering by the tissue. These components are high-energy, but low-volume in percentage total power.

This research programme has been aided by stimulating discussions with A. Brush, M. Barfield, G. Barrowclough, R. Gomulkiewicz, A. Miller, P. Stettenheim and D. Winkler. We are especially grateful for comments on scattering physics from C. F. Bohren. The manuscript was substantially improved by criticisms from three anonymous reviewers. R. Gomulkiewicz and J. Vogel kindly helped with an earlier attempt at 1D Fourier analysis of feather barbs. Feather specimens were supplied by the University of Kansas Natural History Museum (KU) Division of Ornithology. We are thankful to Tim Buller and the University of Kansas Department of Mathematics for computing assistance. This research was supported by grants from the National Science Foundation to R.O.P. (DEB-9318273) and R.H.T. (DMS-9696267).

REFERENCES

Andersson, S. 1996 Bright ultraviolet colouration in the Asian whistling-thrushes (*Myiophonus* spp.). *Proc. R. Soc. Lond.* B **263**, 843–848.

Andersson, S. 1998 Morphology of UV reflectance in a whistling-thrush: implications for the study of structural colour signalling in birds. *J. Avian Biol.* **29**. (In the press.)

Auber, L. 195. The structures producing 'non-iridescent' blue color in bird-feathers. *Proc. Zool. Soc. Lond.* **129**, 455–486.

Bagnara, J. T. & Hadley, M. E. 1973 *Chromatophores and color change.* New Jersey: Prentice Hall.

Benedek, G. B. 1971 Theory of transparency of the eye. *Appl. Optics* **10**, 459–473.

Bohren, C. F. & Huffman, D. R. 1983 *Absorption and scattering of light by small particles.* New York: Wiley.

Briggs, W. L. & Henson, V. E. 1995 *The DFT.* Philadelphia, PA: Society for Industrial and Applied Mathematics.

Durrer, H. 1962 Schillerfarben beim Pfau (*Pavo cristatus* L.). *Verh. Naturf. Ges. Basel* **73**, 204–224.

Durrer, H. 1986 The skin of birds: colouration. In *Biology of the integument*. 2. *Vertebrates* (ed. J. Bereiter-Hahn, A. G. Matoltsky & K. S. Richards), pp. 239–247. Berlin: Springer.

Durrer, H. & Villiger, W. 1966 Schillerfarben der Trogoniden. *J. Ornithol.* **107**, 1–26.

Durrer, H. & Villiger, W. 1970 Schilleradien des Goldkuckucks. *Z. Zellforsch.* **109**, 407–413.

Dyck, J. 1971*a* Structure and spectral reflectance of green and blue feathers of the lovebird (*Agapornis roseicollis*). *Biol. Skr.* (*Copenhagen*) **18**, 1–67.

Dyck, J. 1971*b* Structure and colour-production of the blue barbs of *Agapornis roseicollis* and *Cotinga maynana*. *Z. Zellforsch.* **115**, 17–29.

Dyck, J. 1976 Structural colours. *Proc. Int. Ornithol. Congr.* **16**, 426–437.

Dyck, J. 1978 Olive green feathers: reflection of light from the rami and their structure. *Anser, Suppl.* **3**, 57–75.

Dyck, J. 1987 Structure and light reflection of green feathers of fruit doves (*Ptilinopus* spp.) and an Imperial Pigeon (*Ducula concinna*). *Biol. Skr. (Copenhagen)* **30**, 2–43.

Finger, E. 1995 Visible and UV coloration in birds: Mie scattering as the basis of color production in many bird feathers. *Naturwissenschaften* **82**, 570–573.

Finger, E., Burkhardt, D. & Dyck, J. 1992 Avian plumage colors: origin of UV reflection in a black parrot. *Naturwissenschaften* **79**, 187–188.

Fox, D. L. 1976 *Animal biochromes and structural colors*. Berkeley, CA: University of California Press.

Gisselberg, M., Clark, J. I., Vaezy, S. & Osgood, T. 1991 A quantitative evaluation of Fourier components in transparent and opaque calf cornea. *Am. J. Anat.* **191**, 408–418.

Häcker, V. & Meyer, G. 1902 Die blaue Farbe der Voelfedern. *Zool. Jb., Abt. Syst. Geog. Biol. Tiere* **15**, 267–294.

Land, M. F. 1972 The physics and biology of animal reflectors. *Prog. Biophys. Molec. Biol.* **24**, 77–106.

Lee, D. W. 1997 Iridescent blue plants. *Am. Scient.* **85**, 56–63.

Lucas, A. M. & Stettenheim, P. R. 1972 *Avian anatomy—integument*. Washington, DC: US Department of Agriculture.

Macleod, H. A. 1986 *Thin-film optical filters*. Bristol: Adam Hilger.

Parker, A. R., McKenzie, D. R. & Large, M. C. J. 1998 Multilayer reflectors in animals using green and gold beetles as constrasting examples. *J. Exp. Biol.* **201**, 1307–1313.

Prum, R. O., Morrison, R. L. & Ten Eyck, G. R. 1994 Structural color production by constructive reflection from ordered collagen arrays in a bird (*Philepitta castanea*: Eurylaimidae). *J. Morphol.* **222**, 61–72.

Prum, R. O., Torres, R. H., Williamson, S. & Dyck, J. 1998 Constructive interference of light by blue feather barbs. *Nature* **396**, 28–29.

Raman, C. V. 1935 The origin of colours in the plumage of birds. *Proc. Indian Acad. Sci.* A **1**, 1–7.

Thompson, C. M. & Shure, L. 1995 *MATLAB image processing toolbox user's guide*. Natick, MA: The MathWorks.

Vaezy, S. & Clark, J. I. 1991 A quantitative analysis of transparency in the human sclera and cornea using Fourier methods. *J. Microsc.* **163**, 85–94.

Vaezy, S. & Clark, J. I. 1993 Quantitative analysis of the microstructure of the human cornea and sclera using 2-D Fourier methods. *J. Microsc.* **175**, 93–99.

Vaezy, S. & Clark, J. I. 1995 Characterization of the cellular microstructure of ocular lens using 2D power law analysis. *Annls Biomed. Eng.* **23**, 482–490.

Vaezy, S., Smith, L. T., Milaninia, A. & Clark, J. I. 1995 Two-dimensional Fourier analysis of electron micrographs of human skin for quantification of the collagen fiber organization in the dermis. *J. Electron Microsc.* **44**, 358–364.

van de Hulst, H. C. 1981 *Light scattering by small particles*. New York: Dover.

Young, A. T. 1982 Rayleigh scattering. *Physics Today* **35**, 42–48.

As this paper exceeds the maximum length normally permitted, the authors have agreed to contribute to production costs.